THE JOURNAL OF BIOLOGICAL CHEMISTRY VOL. 288, NO. 50, pp. 35749–35757, December 13, 2013

Histone H4 Promotes Prothrombin Autoactivation*

Received for publication, August 12, 2013, and in revised form, October 28, 2013 Published, JBC Papers in Press, October 30, 2013, DOI 10.1074/jbc.M113.509786

Sergio Barranco-Medina[1], **Nicola Pozzi**[1], **Austin D. Vogt, and Enrico Di Cera**[2]

From the Edward A. Doisy Department of Biochemistry and Molecular Biology, Saint Louis University School of Medicine, St. Louis, Missouri 63104

Background: The molecular origin of the prothrombotic properties of histones is unknown.
Results: Histone H4 interacts with prothrombin and promotes autoactivation.
Conclusion: The prothrombotic properties of histone H4 are due to direct interaction with prothrombin.
Significance: Prothrombin autoactivation has pathophysiological relevance.

Recent studies have documented the ability of prothrombin to spontaneously convert to the mature protease thrombin when Arg-320 becomes exposed to solvent for proteolytic attack upon mutation of residues in the activation domain. Whether prothrombin autoactivation occurs in the wild-type under conditions relevant to physiology remains unknown. Here, we report that binding of histone H4 to prothrombin under physiological conditions generates thrombin by autoactivation. The effect is abrogated by mutation of the catalytic Ser-525 and requires the presence of the Gla domain. Fluorescence titrations document direct binding of histone H4 to prothrombin with an affinity in the low nM range. Stopped flow data and luminescence resonance energy transfer measurements indicate that the binding mechanism obeys conformational selection. Among the two conformations of prothrombin, collapsed and fully extended, histone H4 binds selectively to the collapsed form and induces a transition toward a new conformation where the distance between Ser-101 in kringle-1 and Ser-210 in kringle-2 increases by 13 Å. These findings confirm the molecular plasticity of prothrombin emerged from recent structural studies and suggest that different conformations of the inter-kringle linker domain determine the functional behavior of prothrombin. The results also broaden our mechanistic understanding of the prothrombotic phenotype observed during cellular damage due to the release of histones in the blood stream. Prothrombin autoactivation induced by histone H4 emerges as a mechanism of pathophysiological relevance through which thrombin is generated independently of activation of the coagulation cascade.

Prothrombin, or coagulation factor II, is a 579-residue-long vitamin K-dependent zymogen that circulates in the blood at a concentration of 0.1 mg/ml (1). The protein has a multidomain structure comprising fragment 1 containing the Gla domain and kringle-1, fragment 2 containing kringle-2, and the protease domain containing the A chain and the catalytic B chain. In the penultimate step of the coagulation cascade, prothrombin is proteolytically converted to the active protease thrombin by the prothrombinase complex composed of the protease factor Xa and the cofactor Va assembled on the surface of platelets in the presence of Ca^{2+} (2). The conversion involves cleavage at two residues: Arg-271 located in a linker region connecting kringle-2 to the A chain and Arg-320 in the activation domain of the A chain. Cleavage at Arg-271 sheds fragment 1 and fragment 2 and generates the inactive precursor prethrombin-2. The alternative cleavage at Arg-320 separates the A and B chains that remain connected through a disulfide bond and yields the active intermediate meizothrombin. Under physiological conditions on the surface of platelets, activation of prothrombin proceeds via the prethrombin-2 intermediate (3, 4). The recent crystal structure of prothrombin supports this preferred pathway of activation based on the different solvent accessibility of the two sites of cleavage and the distinct electrostatic properties of the epitope recognizing factor Xa in prothrombin and prethrombin-2 (5). Of particular importance is the observation that Arg-320 in the activation domain is not accessible to proteolysis in solution. Burial of Arg-320 acts as a safety mechanism to prevent prothrombin autoactivation (6) and directs prothrombinase to cleave at Arg-271 first to generate thrombin via the inactive prethrombin-2 intermediate.

The recently discovered property of prothrombin and other inactive thrombin precursors prethrombin-1 and prethrombin-2 to autoactivate has mechanistic significance. Mutations in the activation domain of prethrombin-2, prethrombin-1, and prothrombin that expose Arg-320 to solvent elicit a spontaneous conversion of the zymogen to the mature protease. The conversion typically unfolds over several hours, but in some cases, it is extremely rapid and completes during purification (6). The conversion is initiated by the zymogen itself by virtue of the pre-existing equilibrium between inactive (E*) and active (E) forms (7) and is then propagated and amplified by the mature enzyme. Whether autoactivation takes place in the wild-type protein under the influence of specific cofactors, as observed in other zymogens (8, 9), remains an unresolved issue of potential physiological significance because it would afford a mechanism of thrombin generation that bypasses activation of the coagulation cascade. Cofactor-induced autoactivation represents an alternative strategy for thrombin generation compared with that used by *Staphylococcus aureus*, an important human pathogen implicated in sepsis and endocarditis, whose cofactor staphylocoagulase activates prothrombin by inserting its N-terminal peptide into the activation pocket to allosteri-

* This work was supported in part by National Institutes of Health Research Grants HL49413, HL73813, and HL112303.
[1] Both authors contributed equally to this work.
[2] To whom correspondence should be addressed: Dept. of Biochemistry and Molecular Biology, Saint Louis University School of Medicine, St. Louis, MO 63104. Tel.: 314-977-9201; Fax: 314-977-9206; E-mail: enrico@slu.edu.

cally induce a functional catalytic triad without cleaving at Arg-320 (10). We therefore screened a number of molecules relevant to blood pathophysiology for the ability to specifically promote prothrombin autoactivation.

During cell necrosis, a broad range of modulators such as polyamines, RNA, and histones are released into the extracellular media where they interact with many players of inflammation, sepsis, and thrombosis. Direct administration of histones to mice elicits lethal prothrombotic responses, thereby suggesting a direct link with clotting factors (11). Histones promote activation of factor VII activating protease *in vivo* (8) and have been suggested to interact with fibrinogen (12, 13), prothrombin (12), thrombomodulin, and protein C (14). Histones have been postulated to enhance thrombin generation indirectly by reducing the thrombomodulin-dependent activation of protein C anticoagulant pathway (14) or directly through platelet dependent mechanisms involving the Toll-like receptors TLR2 and TLR4 (15). Here, we show that histone H4 promotes prothrombin autoactivation by interacting directly with the zymogen, and we elucidate the underlying mechanism. The results broaden our understanding of the prothrombotic role of histone H4 and offer the first example of a physiological cofactor of prothrombin autoactivation.

MATERIALS AND METHODS

Numbering—All prothrombin residues in this study are numbered sequentially based on the sequence of the zymogen. The corresponding number according to chymotrypsinogen for residues in the protease domain (A and B chains) is noted by parentheses, *e.g.* the catalytic Ser is identified as Ser-525 (Ser-195).

Materials—Recombinant full-length prothrombin (residues 1–579) wild-type and mutants S525A (S195A) and S101C/S210C, Gla domainless prothrombin (residues 45–579) and prethrombin-1 were cloned into the pNUT vector using restriction sites HindIII and NdeI, transfected into baby hamster kidney cells by lipofection and selected by methotrexate. Prethrombin-2 wild-type and mutant S195A were cloned into the pET-21-b vector using the same restriction enzymes and expressed in *Escherichia coli* as described elsewhere (16). The nucleotide sequence of the constructs was confirmed by DNA sequencing. Addition of vitamin K to the full-length prothrombin media ensured correct γ-carboxylation of the Gla domain. Purification of the recombinant proteins was carried out by affinity chromatography, ion exchange chromatography, and size exclusion chromatography, as described previously (16–20). Homogeneity and chemical identity of final preparations were verified by SDS-PAGE and by RP-HPLC mass spectrometry analysis, giving a purity of >98%. Recombinant histone H3 and histone H4 were purchased from New England Biolabs. Histones were thawed and buffer exchanged immediately before use. Long-chain synthetic polyphosphate was differentially solubilized as described previously (21). Polymer lengths ranged from ~50 to 1500 phosphates, with a modal length of ~650 phosphates. Polyphosphate concentration was expressed in terms of the concentration of phosphate monomers (monomer formula, $NaPO_3$). Spermidine was purchased from Sigma-Aldrich. Protein concentrations were determined by reading at 280 nm with molar extinction coefficients $\epsilon = 111{,}280\ \text{M}^{-1}\ \text{cm}^{-1}$ for recombinant prothrombin (molecular mass, 72,000 kDa) and $\epsilon = 5{,}120\ \text{M}^{-1}\ \text{cm}^{-1}$ for histone H4 (molecular mass, 11237 kDa).

Autoactivation of Prothrombin—Prothrombin at physiological concentration (0.1 mg/ml) was incubated at 37 °C with spermidine (40 μM), RNA (10 μg/ml), DNA (10 μg/ml), polyphosphate (10 μM), and histones H3 and H4 (2 μM) in buffer containing 150 mM NaCl, 5 mM $CaCl_2$, 20 mM Tris, pH 7.4 (TBS-Ca^{2+}). Prothrombin autoactivation was followed for up to 150 h. The reaction leading to generation of mature enzyme and depletion of zymogen was quenched at different times with 15 μl of NuPAGE LDS buffer containing β-mercaptoethanol as reducing agent. Samples were processed by SDS-PAGE. Gels were stained with Coomassie Brilliant Blue R-250. Identity of the bands was confirmed by N-terminal sequencing. The same samples were tested for activity using the thrombin specific chromogenic substrate H-D-Phe-Pro-Arg-*p*-nitroanilide (FPR). The release of *p*-nitroanline was followed at 405 nm, and the amount of active enzyme was quantified with a standard reference curve.

Fluorescence Titration Studies—The prothrombin mutant S101C/S210C was labeled with Alexa Fluor 647 after selective reduction of the engineered cysteines as described elsewhere (5). The labeled protein was separated from the unreacted dye and aggregates by size exclusion chromatography. Incorporation of the probe was confirmed by reading at 650 nm where Alexa Fluor 647 absorbs with an extinction coefficient $\epsilon = 239{,}000\ \text{M}^{-1}\ \text{cm}^{-1}$. The derivatization yield at the two sites was estimated by the ratio of readings at 280/650 nm and found to be 91%. The labeled mutant was tested in the prothrombinase complex assay and returned kinetic parameters comparable with the recombinant wild-type and plasma prothrombin (data not shown). Titration measurements were performed in a 300-μl cuvette at a protein concentration of 5, 20, or 200 nM in the presence of 150 mM NaCl, 5 mM $CaCl_2$, 0.1% PEG 8000, 20 mM Tris, pH 7.4, at 25 °C. The protein was excited at 650 nm (slits 5/10, exposure time of 0.02 s), and the emission spectrum was recorded between 660 and 750 nm. No photobleaching was observed under these conditions. Measurements were perfomed on a Fluoromax-4 spectrofluorimeter (Horiba Scientific, Edison, NJ) and analyzed with Origin (version 8.1, OriginLab, Northampton, MA) using Equation 1,

$$F = F_0 + \Delta F_{\max}\theta \qquad \text{(Eq. 1)}$$

where F is the fluorescence reading, F_0 is the value of F in the absence of histone H4, $\Delta F_{\max}$ is the total change in fluorescence upon saturation, and

$$\theta = \frac{K_{d,\text{app}} + Np_t + h_t - \sqrt{(K_{d,\text{app}} + Np_t + h_t)^2 - 4Np_th_t}}{2Np_t} \qquad \text{(Eq. 2)}$$

Equation 2 shows the fractional saturation defined in terms of the apparent equilibrium dissociation constant, $K_{d,\text{app}}$, the total concentrations of prothrombin, p_t, and histone H4, h_t, and the histone H4:prothrombin stoichiometry N. Histone H4 binding curves obtained at different values of p_t were analyzed simultaneously to derive the independent parameters $K_{d,\text{app}}$ and N.

Stopped Flow Studies—Stopped flow fluorescence measurements were carried out with an Applied Photophysics SX20 spectrometer, using an excitation of 650 nm and a cutoff filter at 665 nm. Samples of prothrombin mutant S101C/S210C labeled with Alexa Fluor 647 at a final concentration of 20 nM were mixed 1:1 with 60-μl solutions of the same buffer (150 mM NaCl, 0.1% PEG 8000, 50 mM Tris, pH 7.4, at 25 °C) containing variable concentrations of histone H4. Each trace was determined in quadruplicate. A base line, established by mixing 20 nM prothrombin with buffer in a 1:1 ratio, was subtracted from each kinetic trace to control negligible amounts of photodegradation. Fits to single and double exponential equations were carried out using software provided by Applied Photophysics. Final k_{obs} values were taken as the average from a minimum of three independent titrations. Two independent relaxations were detected as a function of histone H4 concentration, and the resulting k_{obs} values were fit simultaneously using Mathematica (version 9.0.1.0) to the conformational selection mechanism (22, 23),

$$\mathrm{ProT_1} \underset{k_{12}}{\overset{k_{21}}{\rightleftharpoons}} \mathrm{ProT_2} \underset{k_{on}[H4]}{\overset{k_{off}}{\rightleftharpoons}} \mathrm{ProT_2{:}H4}$$

SCHEME 1

where k_{on} (M^{-1} s^{-1}) is the second-order rate constant for histone H4 binding and k_{off} (s^{-1}) is the first-order rate of dissociation of the complex into the parent species. The strength of the interaction is quantified by the equilibrium dissociation constant K_d (M) defined as the ratio k_{off}/k_{on}. The species $ProT_1$ and $ProT_2$ denote two pre-existing conformations of prothrombin with histone H4 binding exclusively to $ProT_2$. The rate constants k_{12} and k_{21} refer to the transitions from $ProT_1$ to $ProT_2$ and backward, with the ratio $r = k_{21}/k_{12}$ quantifying the population of $ProT_1$ relative to $ProT_2$. The apparent equilibrium dissociation constant, $K_{d,app}$ associated with Scheme 1, is given by the linkage relationship (22) shown in Equation 3,

$$K_{d,app} = \frac{k_{off}}{k_{on}}\left(1 + \frac{k_{21}}{k_{12}}\right) = K_d(1 + r) \qquad \text{(Eq. 3)}$$

which indicates that the value measured experimentally always overestimates the intrinsic equilibrium dissociation constant, K_d, for the interaction.

Luminescence Resonance Energy Transfer (LRET) Studies—The prothrombin mutant S101C/S210C and its labeled forms with the donor (Eu^{3+})AMCA-DTPA and acceptor Alexa Fluor 647 were prepared as described in detail elsewhere (5). LRET[3] measurements were performed with a custom-built two-channel spectrofluorometer with a pulsed nitrogen laser (NL100, Stanford Research Systems, Sunnyvale, CA) as an excitation source (24). Measurements were performed in a 300-μl cuvette in 20 mM Tris, 150 mM NaCl, 5 mM $CaCl_2$, 0.1% PEG 8000, pH 7.4 at 37 °C. The concentration of labeled proteins was 10–75 nM. Donor emission was recorded at 617 nm using a 620 nm, 10-nm bandwidth interference filter (Oriel, Stratford, CT), and acceptor emission was recorded at 670 nm using a 670 nm, 10 nm bandwidth interference filter (Oriel). Decays for donor-only samples were mono-exponential and were analyzed according to Equation 4,

$$I(t) = A_{exp}(-t/\tau) \qquad \text{(Eq. 4)}$$

where A is the amplitude of the decay and τ is the luminescence lifetime. Decays of donors in the presence of acceptor and decays of sensitized acceptor emission were triple-exponential in the absence or presence of histone H4. Donor and sensitized acceptor decay curves were fitted simultaneously using global nonlinear regression with Origin (version 8.1). The energy transfer (E) was calculated from measurements of luminescence lifetime of the donor in the absence (τ_d) and presence of acceptor (τ_{da}) as shown in Equation 5.

$$E = \frac{\tau_d - \tau_{da}}{\tau_d} \qquad \text{(Eq. 5)}$$

The distance R between donor and acceptor was calculated according to the Förster equation below,

$$R^6 = R_0^6 \frac{1 - E}{E} = R_0^6 \frac{\tau_{da}}{\tau_d - \tau_{da}} \qquad \text{(Eq. 6)}$$

where R_0 is the distance where the energy transfer $E = 0.5$ (50%) and is equal to 55 Å for a completely randomized orientation of the donor-acceptor pair used (24, 25).

RESULTS

During response to traumatic injury, sepsis, inflammation, and cell necrosis, the levels of histones, RNA, and polyamines become elevated in the blood (8, 9, 11, 14, 15, 26) and correlate with thrombosis, inflammation, and multiple organ dysfunction (27, 28). We explored the possibility that some of these components express their prothrombotic function via direct interaction with prothrombin. Autoactivation of prothrombin at physiological concentration (0.1 mg/ml) was monitored following incubation with histone H3, histone H4, spermidine, polyphosphate, RNA, or DNA, mindful of the autoactivation effects elicited by some of these molecules on other zymogens (29). Histone H4 was unique in promoting conversion of prothrombin to the mature protease thrombin and produced three new bands in SDS electrophoresis (Fig. 1), similar to the results recently obtained upon mutations of the activation domain leading to exposure of Arg-320 and autoactivation (6). N-terminal sequencing identified these new bands as prethrombin-1, prethrombin-2, and fragment 1.2. Prothrombin samples incubated with histone H4 at different time intervals showed increasing activity levels against the thrombin specific chromogenic substrate FPR (Fig. 1). Control experiments with prothrombin without histone H4 or the prothrombin mutant S525A (S195A) in the presence of histone H4 failed to show autoactivation (Fig. 1), ruling out contamination of the sample with trace amounts of thrombin or other proteases. The control with prothrombin S525A (S195A), with the catalytic Ser replaced by Ala, indicates that autoactivation is initiated by prothrombin itself through the intrinsic activity of the zymogen. This was confirmed by a strong dependence of autoactivation

[3] The abbreviation used is: LRET, luminescence resonance energy transfer.

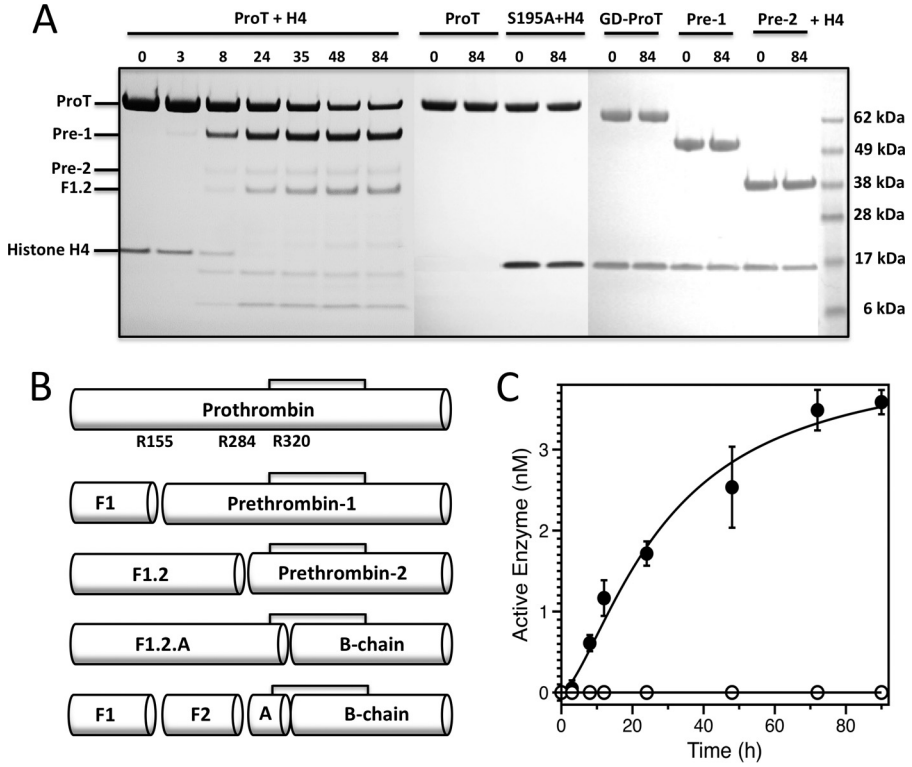

FIGURE 1. **Histone H4 promotes autoactivation of prothrombin under physiological conditions.** *A*, prothrombin (0.1 mg/ml) was incubated with histone H4 (2 μM) in 150 mM NaCl, 5 mM $CaCl_2$, 20 mM Tris, pH 7.4, at 37 °C, and the reaction was followed by SDS-PAGE under reducing conditions as a function of time as indicated (h). The generation of thrombin was confirmed by cleavage of prothrombin (*ProT*) at Arg-155 and Arg-284 to generate the intermediates prethrombin-1 (*Pre-1*, 50 kDa, N-terminal sequence detected SEGSS) and prethrombin-2 (*Pre-2*, 38 kDa, N-terminal sequence detected TFGSG), respectively, as revealed by N-terminal sequencing. A third lower band was also identified by N-terminal sequencing and assigned to fragment 1.2 (*F1.2*, 34 kDa, N-terminal sequence detected ANTFL). Autoactivation requires histone H4, the catalytic Ser-525 (*S195*) and the Gla domain, because it is not observed in Gla domainless prothrombin (*GD-ProT*), prethrombin-1 or prethrombin-2. Cleavage of histone H4 by thrombin explains why autoactivation does not reach completion even after 84 h. *B*, schematic representation of prothrombin and its auto-proteolytic products upon incubation with histone H4. Cleavage at Arg-155 generates prethrombin-1 (*Pre-1*) and fragment 1 (*F1*). Cleavage at Arg-284 produces prethrombin-2 (*Pre-2*) and fragment 1.2 (*F1.2*), and additional cleavage of prethrombin-2 at Arg-320 generates the A and B chains of the mature enzyme thrombin. Direct cleavage of Arg-320 generates the B chain and fragment 1.2.A (*F1.2.A*) of meizothrombin, where fragment 1.2 remains attached to the A chain. *C*, formation of active enzyme confirmed by spectrophotometric analysis. Time point aliquots of the prothrombin autoactivation experiments were tested for activity toward the thrombin specific chromogenic substrate FPR (*filled circles*). Initial velocities were transformed in concentrations by using a thrombin standard curve. No activity was detected in the absence of histone H4 (*open circles*).

on the prothrombin concentration, as expected for a reaction initiated by the zymogen itself as a catalyst (data not shown). Histone H3 also promoted autoactivation but over a time scale three times longer than that observed with histone H4 (data not shown), in agreement with the observation that the procoagulant effect of histones is due mainly to histone H4 (14).

Previous studies have shown a requirement for the Gla domain in the binding of histones to vitamin K-dependent proteins (12, 14). Accordingly, autoactivation of prothrombin by histone H4 required the presence of the Gla domain and was not observed with Gla domainless prothrombin, or the thrombin precursors prethrombin-1 and prethrombin-2 that lack fragment 1 or both fragments 1 and 2 (Fig. 1), respectively.

The disappearance of the band corresponding to histone H4 in the gel during prothrombin autoactivation was due to proteolytic cleavage by the mature enzyme thrombin because no degradation was observed with prothrombin S525A (S195A). Activated protein C is currently the only enzyme known to target histones in the blood and able to counter their prothrombotic effects and cytotoxicity (11). The uniqueness of this effect should be reconsidered in view of the data reported in Fig. 1. The ability of thrombin to degrade histone H4 explains why prothrombin autoactivation does not proceed to completion (Fig. 1).

The evidence that histone H4 interacts with prothrombin is compelling but indirect. Histones are positively charged and may interact non-specifically with the surface of prothrombin that is mostly negatively charged, as recently revealed by the x-ray crystal structure (5). Evidence of a direct interaction of histone H4 with prothrombin comes from fluorescence titrations using the prothrombin mutant S101C/S210C engineered recently for quantitative LRET measurements (5). The mutant labeled with the dye Alexa Fluor 647 at both Cys residues was used first for direct fluorescence titrations (Fig. 2). Upon interaction with histone H4, the fluorescence of prothrombin decreases 30% and produces binding curves with an apparent equilibrium dissociation constant $K_{d,\mathrm{app}} = 9 \pm 1$ nM and a stoichiometry $N = 1.2 \pm 0.1$ indicating binding to a single site. Binding of histone H4 is reversed completely by addition of heparin that is known to interact strongly with histones (30).

Information on the mechanism of interaction of histone H4 with prothrombin was obtained from rapid kinetics measurements. Binding of histone H4 to the prothrombin mutant S101C/S210C labeled with Alexa Fluor 647 induces a significant fluorescence change consistent with a double exponential

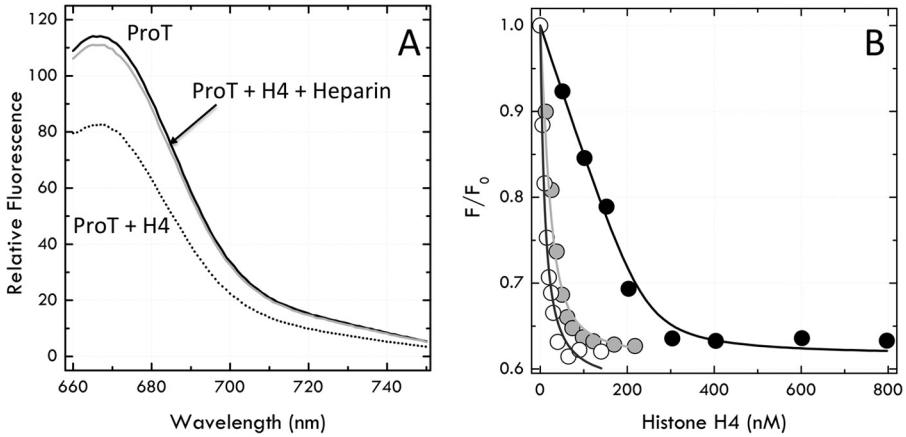

FIGURE 2. **Histone H4 binding to prothrombin.** *A*, prothrombin mutant S101C/S210C (20 nM) labeled with Alexa Fluor 647 at both Cys residues was excited at 650 nm in the absence (*solid line*) or presence (*dotted line*) of 0.5 μM histone H4. Upon complex formation, the fluorescence intensity decreases 30%. Addition of 3.5 μM unfractioned heparin (*gray solid line*) neutralizes the effect of histone H4 and restores the original spectrum of prothrombin. *B*, histone H4 binds to prothrombin to a single site ($N = 1.2 \pm 0.2$) with an apparent equilibrium dissociation constant $K_{d,app} = 9 \pm 1$ nM. Data refer to three different prothrombin concentrations (5 nM, *open circles*; 20 nM, *gray circles*; 200 nM, *black circles*) and are plotted as intrinsic fluorescence *F* normalized by F_0 to facilitate comparison. Data were analyzed simultaneously according to Equations 1 and 2 in the text with eight independent parameters and best fit values: $K_{d,app} = 9 \pm 1$ nM, $N = 1.2 \pm 0.2$ and (*open circles*), $F_0 = 2.1 \pm 0.1$ MV (1 MV = 10^6 volts); $\Delta F_{max} = -0.86 \pm 0.02$ MV (*gray circles*); $F_0 = 6.6 \pm 0.1$ MV, $\Delta F_{max} = -2.6 \pm 0.1$ MV; (*black circles*) $F_0 = 12 \pm 1$ MV, $\Delta F_{max} = -4.8 \pm 0.1$. Experimental conditions were as follows: 150 mM NaCl, 5 mM $CaCl_2$, 0.1% PEG8000, 20 mM Tris, pH 7.4, at 25 °C.

relaxation to equilibrium (Fig. 3). Two relaxations accessible to experimental measurements show distinct dependence on the histone H4 concentration (Fig. 3): one is fast and increases linearly at high concentrations, and the other is slow and increases hyperbolically. The concentration dependence of the two relaxations is consistent with a binding mechanism obeying conformational selection (22, 23) as described in Scheme 1: prothrombin undergoes a pre-existing equilibrium between two conformations, $ProT_1$ and $ProT_2$, of which only $ProT_2$ specifically interacts with histone H4. The scenario agrees well with the recent crystal structure of prothrombin documenting conformational flexibility of the zymogen due to extreme mobility of the linker domain connecting kringle-1 and kringle-2 (5). The data in Fig. 3 enable derivation of important parameters for the binding interaction and the linked conformational transitions (22, 23). The slope of the straight line in the fast relaxation gives the second order rate constant of association $k_{on} = 5.5 \pm 0.5\ \mu M^{-1}\ s^{-1}$ and the asymptotic value of the slow relaxation gives the value of $k_{12} = 0.6 \pm 0.2\ s^{-1}$ for the conversion of $ProT_1$ to $ProT_2$. A global fit of the two relaxations to Equation 6 of Ref. 22 yields the remaining parameters in Scheme 1: the rate constant for the reverse $ProT_2$ to $ProT_1$ transition is $k_{21} = 0.5 \pm 0.1\ s^{-1}$, and the rate of dissociation of the complex into the parent species $ProT_2$ and histone H4 is $k_{off} = 0.04 \pm 0.01\ s^{-1}$. These values give a $K_{d,app} = 13 \pm 1$ nM (see Equation 3), which is very close to the value of $K_{d,app} = 9 \pm 1$ nM derived from fluorescence titrations under identical solution conditions (Fig. 2). The two conformations of prothrombin, $ProT_1$ and $ProT_2$, detected by stopped flow are populated as $k_{21}/(k_{12} + k_{21}) = 45\%$ and $k_{12}/(k_{12} + k_{21}) = 55\%$, respectively. Notably, this distribution is similar to that involving the collapsed and fully extended conformations of prothrombin identified recently by LRET measurements (5). However, stopped flow data are unable to address whether $ProT_1$ and $ProT_2$ in Scheme 1 have any connection with the fully extended and collapsed conformations of prothrombin.

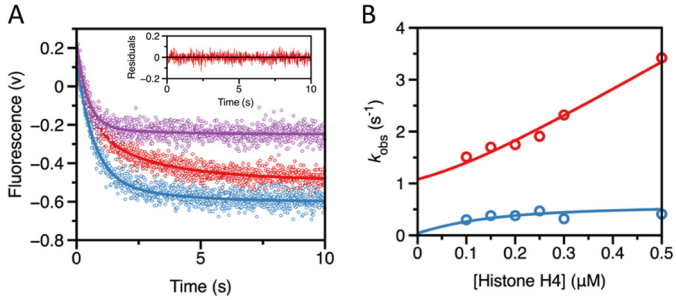

FIGURE 3. **Kinetic mechanism of histone H4 binding to prothrombin.** *A*, kinetic traces in the 0–10-s time scale of histone H4 binding to the prothrombin mutant S101C/S210C labeled with Alexa Fluor 647 at both Cys residues. Shown are the traces obtained by mixing 20 nM prothrombin with 100 nM (*red*), 200 nM (*cyan*), and 300 nM (*magenta*) histone H4. *Solid lines* were drawn according to a double exponential fit. Experimental conditions were as follows: 150 mM NaCl, 0.1% PEG 8000, 50 mM Tris, pH 7.4, at 25 °C. The *inset* gives the distribution of residuals for double exponential fits to the kinetic trace for the mixing of prothrombin with 100 nM histone H4. Double exponential fits rectify deviations from the experimental data present in the single exponential fits. *B*, plots of the two independent relaxations, fast (*red*) and slow (*cyan*), derived from the double exponential fits as a function of histone H4 concentration. *Solid lines* were drawn according to Scheme 1 in the text depicting a conformational selection mechanism, using the expressions in Equation 6 of Ref. 22 with best fit parameter values: $k_{12} = 0.6 \pm 0.2\ s^{-1}$, $k_{21} = 0.5 \pm 0.1\ s^{-1}$, $k_{on} = 5.5 \pm 0.5\ \mu M^{-1} s^{-1}$, and $k_{off} = 0.04 \pm 0.01\ s^{-1}$. The resulting value of the apparent equilibrium dissociation constant, $K_{d,app}$, for this mechanism was derived from Equation 3 in the text as 13 ± 1 nM, in agreement with the value derived from fluorescence titrations under identical solution conditions (see Fig. 2).

To further explore the mechanistic implications of the results from rapid kinetics data, the interaction of histone H4 with prothrombin was investigated by LRET measurements of the mutant S101C/S210C labeled with the donor (Eu^{3+})AMCA-DTPA and acceptor Alexa Fluor 647 as dyes. The recent crystal structure of prothrombin along with LRET measurements have revealed that kringle-1 moves similar to a dumbbell relative to the rest of the zymogen due to the extreme flexibility of the linker connecting the two kringles (5). As a result, prothrombin assumes two alternative conformations in solution: a fully extended conformation with a population of 55% where Ser-101 in kringle-1 and Ser-210 in

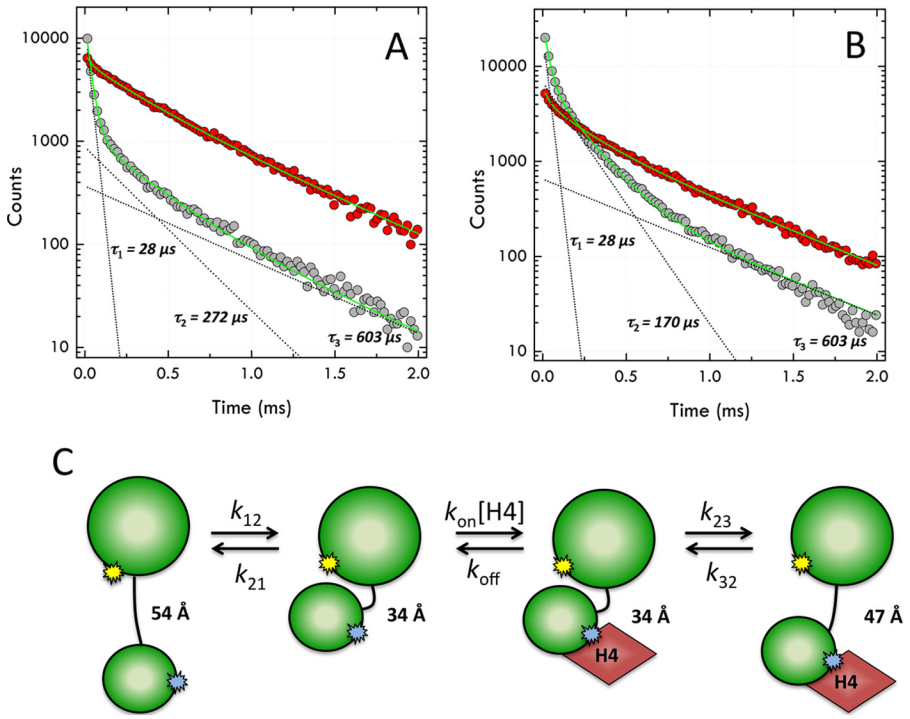

FIGURE 4. **LRET measurements of histone H4 binding to prothrombin.** Semilog plot of lifetime data for the LRET donor-acceptor pair conjugated to residues 101 in kringle-1 and 210 in kringle-2 of the full-length prothrombin mutant S101C/S210C (150 nM) in the absence (*A*) or presence (*B*) of 0.9 μM histone H4. The donor quenching (*red dots*) and acceptor sensitization (*gray dots*) curves of prothrombin both fit to a triple-exponential decay (*green line*) and two populations, collapsed and fully extended (5). Decomposition of the triple exponential fit into its individual components (*dotted lines*) reveals a short relaxation with a lifetime τ_1 = 28 ± 3 μs associated with the collapsed conformation and a longer relaxation with τ_2 = 272 ± 8 μs associated with the fully extended conformation. The third, slowest relaxation with τ_3 = 603 ± 9 μs corresponds to the donor only control. Binding of histone H4 to prothrombin does not alter the short relaxation but selectively perturbs the longer relaxation that is replaced by a shorter decay with a lifetime of 170 ± 5 μs. The amplitudes A_1 for τ_1 and A_2 for τ_2, which define the distribution between the two conformations, also change in favor of the newly generated species bound to histone H4. In the absence of histone H4, the ratio between collapsed and fully extended conformations is 0.85, consistent with the 1.2 ratio measured by stopped-flow for the $ProT_2$:$ProT_1$ distribution (see Fig. 3). In the presence of saturating concentrations of histone H4, the fully extended conformation disappears and the collapsed conformation partially converts to the new conformation to a final 0.35 ratio (collapsed:new). Best fit parameters for the triple-exponential decay curves are as follows: *A*, A_1 = 13,400 ± 200, τ_1 = 28 ± 3 μs; A_2 = 950 ± 20, τ_2 = 272 ± 8 μs; A_3 = 367, τ_3 = 603 ± 9 μs; *B*, A_1 = 22,900 ± 200, τ_1 = 28 ± 3 μs; A_2 = 6950 ± 70, τ_2 = 170 ± 5 μs; A_3 = 650 ± 8, τ_3 = 603 ± 9 μs. Experimental conditions were as follows: 150 mM NaCl, 5 mM $CaCl_2$, 0.1% PEG 8000, 20 mM Tris, pH 7.4, at 37 °C. *C*, proposed mechanism of histone H4 binding to prothrombin based on rapid kinetics and LRET measurements. When free in solution, prothrombin exists in at least two conformations where the distance between Ser-101 in kringle-1 and Ser-210 in kringle-2 is either partially collapsed (≤34 Å, corresponding to $ProT_2$ in Scheme 1) or fully extended (54 Å, corresponding to $ProT_1$ in Scheme 1), as reported recently (5). Histone H4 selectively binds to the collapsed conformation of prothrombin and then induces a conformational change that increases the distance between the two reporters (*yellow* and *cyan stars*) to 47 Å. The donor-acceptor distances were derived from the Föster equation (Equation 6 in the text). The induced fit step in the kinetic mechanism detected by LRET measurements is not detected in the stopped flow measurements (see Fig. 3) because the associated relaxation is spectroscopically silent.

kringle-2 are separated by a distance of 54 ± 2 Å, and a collapsed conformation with a population of 45% where Ser-101 in kringle-1 and Ser-210 in kringle-2 are separated by a distance of ≤34 Å or are at least 20 Å closer than in the fully extended conformation (5). LRET measurements carried out at physiological temperature in the absence or presence of a saturating concentration (0.9 μM) of histone H4 show a drastic effect on the distribution of prothrombin conformers. Three independent relaxations are detected experimentally in each case (Fig. 4). In the absence of histone H4, the slowest lifetime of 603 μs refers to the decay of the donor-only control, the short lifetime of 28 ± 3 μs with 45% population has a distance between Ser-101 in kringle-1 and Ser-210 in kringle-2 of ≤34 Å, and the long lifetime of 272 ± 8 μs with 55% population has a distance of 54 ± 2 Å. These results are practically identical to those reported recently (5). Under saturating concentrations of histone H4 the lifetime of the collapsed conformation remains unchanged, but a new lifetime of 170 ± 5 μs corresponding to a distance between the probes of 47 ± 2 Å replaces the one pertaining to the fully extended conformation. Binding of histone H4 occurs exclusively to the collapsed conformation, followed by an induced fit transition into a new more extended form where the distance between the probes in kringle-1 and kringle-2 increases by 13 Å. LRET measurements enable assignment of $ProT_1$ in Scheme 1 as the fully extended conformation of prothrombin and identify $ProT_2$ with the collapsed conformation. The relative distributions of these two conformations are close to 1:1 based on stopped flow and LRET measurements. Upon binding to $ProT_2$, histone H4 causes prothrombin to assume a new conformation (Fig. 4). The overall mechanism of histone H4 recognition calls for a mixed kinetic scheme where conformational selection is followed by an induced fit step (Fig. 4) that is spectroscopically silent. These findings provide evidence that histone H4 interacts specifically with prothrombin by selecting the collapsed conformation and promoting autoactivation via an induced fit mechanism that optimizes the conformation of the initial prothrombin-histone H4 complex.

DISCUSSION

Recent studies have documented the ability of thrombin precursors prothrombin, prethrombin-1 and prethrombin-2 to autoactivate (6, 16). Autoactivation is started by the zymogen itself because it is specifically abrogated by replacement of the catalytic Ser-525 (Ser-195) with Ala. The reaction is then propagated by thrombin and rapidly amplified (6). Autoactivation is found in other zymogens such as proprotein convertases furin and kexin type 9 (31–33), plasma hyaluronan-binding protein (26), recombinant factor VII (34), and the membrane-bound matriptases (35, 36). The pre-existing equilibrium of the trypsin fold between the E* (inactive) and E (active) forms (7, 37) explains autoactivation in terms of the small intrinsic activity of the zymogen (6). However, in the case of prothrombin, the question remains as to the physiological relevance of autoactivation given that Arg-320 (Arg-15) is not accessible to proteolytic attack in the wild-type (5). The results reported in this study demonstrate that autoactivation of prothrombin can be triggered in the wild-type by histone H4 over a time scale of ~8 h. The effect is slow but physiologically relevant because the high concentration (0.1 mg/ml) of prothrombin in the blood provides a reservoir for continuous thrombin generation by autoactivation. It is also possible that autoactivation *in vivo* unravels under a much shorter time scale because of conditions favoring sequestration of prothrombin by histone H4 or the presence of other cofactors yet to be identified. Other zymogens autoactivate upon interaction with external cofactors. Hyaluronan-binding protein (factor VII activating protease) autoactivates upon binding of histones (8), negatively charged molecules such as heparin and RNA (9, 29, 38–40), and spermidine (41). Coagulation factors XI and XII autoactivate upon binding of RNA (9). Histone H4 specifically requires the Gla domain to promote autoactivation of prothrombin and likely induces exposure of Arg-320 (Arg-15) to solvent via a long range allosteric effect that propagates from the Gla domain to the activation domain situated nearly 80 Å away (5). The effect is mechanistically relevant and draws attention to the presence of long range communication within the prothrombin molecule mediated by the extreme flexibility of its structure (5).

Fluorescence and LRET measurements show that histone H4 binds selectively to the collapsed conformation of the zymogen with an affinity in the low nM range and induces a new conformation where the distance between Ser-101 in kringle-1 and Ser-210 in kringle-2 increases from ≤34 to 47 Å. The new conformation is distinct from the fully extended form of prothrombin where the same distance is 54 Å (5). Histone H4 binds to prothrombin according to a kinetic mechanism that includes conformational selection and induced fit (Fig. 4), a highly versatile scheme whose properties span the entire landscape allowed for independent relaxations (23). The conformational selection component of the kinetic mechanism is supported by stopped flow measurements where histone H4 binds selectively to one of the two possible pre-existing conformations of prothrombin. The result is mechanistically important because it reinforces the notion that trypsin-like zymogens exist in multiple conformations as probed by binding to the active site (16) or auxiliary domains such as the Gla domain reported here. Whether a linkage exists in prothrombin between the E*-E equilibrium affecting the active site region (7, 37, 42) and the equilibrium between the collapsed and fully extended conformations made possible by the flexibility of the linker between kringle-1 and kringle-2 (5) remains to be established. The possibility is intriguing as it suggests a long range communication between the catalytic domain of the zymogen and its auxiliary domains, thereby offering a much needed structural perspective on the mechanism of prothrombin activation.

Because histone H4 promotes autoactivation, we speculate that the new conformation produced by induced fit from the original collapsed form exposes Arg-320 (Arg-15) to solvent for proteolytic attack and stabilizes the active site in the E form. In this context, it becomes of interest to ponder what conformation of prothrombin is stabilized upon interaction with the prothrombinase complex and whether the selection depends on the environment in which prothrombin activation takes place. Based on the results reported here, the fully extended conformation of prothrombin is not prone to autoactivation and may be the one stabilized by assembly of the prothrombinase complex on the surface of platelets, thereby making cleavage at Arg-271 preferred over cleavage at Arg-320 under conditions relevant to physiology (3, 4). On the other hand, conditions where factor Xa and cofactor Va induce conformational transitions in prothrombin similar to those induced by histone H4 may direct cleavage at Arg-320 and promote thrombin generation along the meizothrombin pathway, where cleavage at Arg-320 precedes cleavage at Arg-271 (1). In this scenario, selection between the two sites of cleavage at Arg-271 or Arg-320 would depend on their solvent accessibility and on the conformation of the linker domain between kringle-1 and kringle-2.

The induced fit component of the kinetic mechanism of histone H4 recognition also deserves attention. Stopped flow data do not detect such component, but that may be due to a lack of spectroscopic signal associated with it. Alternatively, the induced fit component may be a simplification of a more general mechanism where the new conformation stabilized by histone H4 binding to the collapsed form actually pre-exists in solution but in minuscule amounts. A mechanism where the pre-existing equilibrium includes such conformation present only as 1% of the total population would fit adequately the LRET data in Fig. 4 and the stopped flow data in Fig. 3, thereby obviating the need for induced fit. This argument is in line with the recent conclusion that conformational selection is always sufficient and induced fit is never necessary as a mechanism of ligand binding (23). Conclusive assessment of the role of induced fit in prothrombin function will require measurements of the underlying conformational transitions at the single molecule level.

The results reported here broaden our understanding of the prothrombotic activity of histones in the context of the well established link between inflammation and thrombosis (28). Infusion of intravenous histones into mice causes sepsis, thrombosis, and death (11). The concentration of histones in the blood reaches 20 μM under pathological conditions (43) and is sufficient to saturate prothrombin and promote autoactivation leading to thrombin generation within few hours. Pro-

longed exposure to histone H4 is equivalent to a slow infusion of small amounts of thrombin in the circulation, which eventually culminates in prothrombotic and proinflammatory effects (28). Prothrombin autoactivation induced by endogenous cofactors such as histone H4 or other mediators of inflammation yet to be identified demonstrates that thrombin can be generated by a mechanism that bypasses activation of the blood coagulation cascade.

REFERENCES

1. Butenas, S., van't Veer, C., and Mann, K. G. (1999) "Normal" thrombin generation. *Blood* **94,** 2169–2178
2. Rosing, J., Tans, G., Govers-Riemslag, J. W., Zwaal, R. F., and Hemker, H. C. (1980) The role of phospholipids and factor Va in the prothrombinase complex. *J. Biol. Chem.* **255,** 274–283
3. Wood, J. P., Silveira, J. R., Maille, N. M., Haynes, L. M., and Tracy, P. B. (2011) Prothrombin activation on the activated platelet surface optimizes expression of procoagulant activity. *Blood* **117,** 1710–1718
4. Haynes, L. M., Bouchard, B. A., Tracy, P. B., and Mann, K. G. (2012) Prothrombin activation by platelet-associated prothrombinase proceeds through the prethrombin-2 pathway via a concerted mechanism. *J. Biol. Chem.* **287,** 38647–38655
5. Pozzi, N., Chen, Z., Gohara, D. W., Niu, W., Heyduk, T., and Di Cera, E. (2013) Crystal structure of prothrombin reveals conformational flexibility and mechanism of activation. *J. Biol. Chem.* **288,** 22734–22744
6. Pozzi, N., Chen, Z., Zapata, F., Niu, W., Barranco-Medina, S., Pelc, L. A., and Di Cera, E. (2013) Autoactivation of thrombin precursors. *J. Biol. Chem.* **288,** 11601–11610
7. Pozzi, N., Vogt, A. D., Gohara, D. W., and Di Cera, E. (2012) Conformational selection in trypsin-like proteases. *Curr. Opin. Struct. Biol.* **22,** 421–431
8. Yamamichi, S., Fujiwara, Y., Kikuchi, T., Nishitani, M., Matsushita, Y., and Hasumi, K. (2011) Extracellular histone induces plasma hyaluronan-binding protein (factor VII activating protease) activation *in vivo*. *Biochem. Biophys. Res. Commun.* **409,** 483–488
9. Kannemeier, C., Shibamiya, A., Nakazawa, F., Trusheim, H., Ruppert, C., Markart, P., Song, Y., Tzima, E., Kennerknecht, E., Niepmann, M., von Bruehl, M. L., Sedding, D., Massberg, S., Günther, A., Engelmann, B., and Preissner, K. T. (2007) Extracellular RNA constitutes a natural procoagulant cofactor in blood coagulation. *Proc. Natl. Acad. Sci. U.S.A.* **104,** 6388–6393
10. Friedrich, R., Panizzi, P., Fuentes-Prior, P., Richter, K., Verhamme, I., Anderson, P. J., Kawabata, S., Huber, R., Bode, W., and Bock, P. E. (2003) Staphylocoagulase is a prototype for the mechanism of cofactor-induced zymogen activation. *Nature* **425,** 535–539
11. Xu, J., Zhang, X., Pelayo, R., Monestier, M., Ammollo, C. T., Semeraro, F., Taylor, F. B., Esmon, N. L., Lupu, F., and Esmon, C. T. (2009) Extracellular histones are major mediators of death in sepsis. *Nat. Med.* **15,** 1318–1321
12. Pemberton, A. D., Brown, J. K., and Inglis, N. F. (2010) Proteomic identification of interactions between histones and plasma proteins: implications for cytoprotection. *Proteomics* **10,** 1484–1493
13. Gonias, S. L., Pasqua, J. J., Greenberg, C., and Pizzo, S. V. (1985) Precipitation of fibrinogen, fibrinogen degradation products and fibrin monomer by histone H3. *Thromb. Res.* **39,** 97–116
14. Ammollo, C. T., Semeraro, F., Xu, J., Esmon, N. L., and Esmon, C. T. (2011) Extracellular histones increase plasma thrombin generation by impairing thrombomodulin-dependent protein C activation. *J. Thromb. Haemost.* **9,** 1795–1803
15. Semeraro, F., Ammollo, C. T., Morrissey, J. H., Dale, G. L., Friese, P., Esmon, N. L., and Esmon, C. T. (2011) Extracellular histones promote thrombin generation through platelet-dependent mechanisms: involvement of platelet TLR2 and TLR4. *Blood* **118,** 1952–1961
16. Pozzi, N., Chen, Z., Zapata, F., Pelc, L. A., Barranco-Medina, S., and Di Cera, E. (2011) Crystal structures of prethrombin-2 reveal alternative conformations under identical solution conditions and the mechanism of zymogen activation. *Biochemistry* **50,** 10195–10202
17. Chen, Z., Pelc, L. A., and Di Cera, E. (2010) Crystal structure of prethrombin-1. *Proc. Natl. Acad. Sci. U.S.A.* **107,** 19278–19283
18. Papaconstantinou, M. E., Gandhi, P. S., Chen, Z., Bah, A., and Di Cera, E. (2008) Na(+) binding to meizothrombin desF1. *Cell Mol. Life Sci.* **65,** 3688–3697
19. Guinto, E. R., Vindigni, A., Ayala, Y. M., Dang, Q. D., and Di Cera, E. (1995) Identification of residues linked to the slow→fast transition of thrombin. *Proc. Natl. Acad. Sci. U.S.A.* **92,** 11185–11189
20. Pozzi, N., Barranco-Medina, S., Chen, Z., and Di Cera, E. (2012) Exposure of R169 controls protein C activation and autoactivation. *Blood* **120,** 664–670
21. Smith, S. A., Choi, S. H., Davis-Harrison, R., Huyck, J., Boettcher, J., Rienstra, C. M., Reinstra, C. M., and Morrissey, J. H. (2010) Polyphosphate exerts differential effects on blood clotting, depending on polymer size. *Blood* **116,** 4353–4359
22. Vogt, A. D., and Di Cera, E. (2012) Conformational selection or induced fit? A critical appraisal of the kinetic mechanism. *Biochemistry* **51,** 5894–5902
23. Vogt, A. D., and Di Cera, E. (2013) Conformational selection is a dominant mechanism of ligand binding. *Biochemistry* **52,** 5723–5729
24. Heyduk, E., and Heyduk, T. (1997) Thiol-reactive, luminescent Europium chelates: luminescence probes for resonance energy transfer distance measurements in biomolecules. *Anal. Biochem.* **248,** 216–227
25. Selvin, P. R., and Hearst, J. E. (1994) Luminescence energy transfer using a terbium chelate: improvements on fluorescence energy transfer. *Proc. Natl. Acad. Sci. U.S.A.* **91,** 10024–10028
26. Yamamoto, E., Kitano, Y., and Hasumi, K. (2011) Elucidation of crucial structures for a catechol-based inhibitor of plasma hyaluronan-binding protein (factor VII activating protease) autoactivation. *Biosci. Biotechnol. Biochem.* **75,** 2070–2072
27. Semeraro, N., Ammollo, C. T., Semeraro, F., and Colucci, M. (2012) Sepsis, thrombosis and organ dysfunction. *Thromb. Res.* **129,** 290–295
28. Esmon, C. T. (2013) Molecular circuits in thrombosis and inflammation. *Thromb. Haemost.* **109,** 416–420
29. Gansler, J., Jaax, M., Leiting, S., Appel, B., Greinacher, A., Fischer, S., and Preissner, K. T. (2012) Structural requirements for the procoagulant activity of nucleic acids. *PLoS One* **7,** e50399
30. Pal, P. K., Starr, T., and Gertler, M. M. (1983) Neutralization of heparin by histone and its subfractions. *Thromb. Res.* **31,** 69–79
31. Gawlik, K., Shiryaev, S. A., Zhu, W., Motamedchaboki, K., Desjardins, R., Day, R., Remacle, A. G., Stec, B., and Strongin, A. Y. (2009) Autocatalytic activation of the furin zymogen requires removal of the emerging enzyme's N-terminus from the active site. *PLoS One* **4,** e5031
32. Artenstein, A. W., and Opal, S. M. (2011) Proprotein convertases in health and disease. *N. Engl. J. Med.* **365,** 2507–2518
33. Piper, D. E., Jackson, S., Liu, Q., Romanow, W. G., Shetterly, S., Thibault, S. T., Shan, B., and Walker, N. P. (2007) The crystal structure of PCSK9: a regulator of plasma LDL-cholesterol. *Structure* **15,** 545–552
34. Sichler, K., Banner, D. W., D'Arcy, A., Hopfner, K. P., Huber, R., Bode, W., Kresse, G. B., Kopetzki, E., and Brandstetter, H. (2002) Crystal structures of uninhibited factor VIIa link its cofactor and substrate-assisted activation to specific interactions. *J. Mol. Biol.* **322,** 591–603
35. Whitcomb, D. C., Gorry, M. C., Preston, R. A., Furey, W., Sossenheimer, M. J., Ulrich, C. D., Martin, S. P., Gates, L. K., Jr., Amann, S. T., Toskes, P. P., Liddle, R., McGrath, K., Uomo, G., Post, J. C., and Ehrlich, G. D. (1996) Hereditary pancreatitis is caused by a mutation in the cationic trypsinogen gene. *Nat. Genet.* **14,** 141–145
36. Stirnberg, M., Maurer, E., Horstmeyer, A., Kolp, S., Frank, S., Bald, T., Arenz, K., Janzer, A., Prager, K., Wunderlich, P., Walter, J., and Gütschow, M. (2010) Proteolytic processing of the serine protease matriptase-2: identification of the cleavage sites required for its autocatalytic release from the cell surface. *Biochem. J.* **430,** 87–95
37. Gohara, D. W., and Di Cera, E. (2011) Allostery in trypsin-like proteases suggests new therapeutic strategies. *Trends Biotechnol.* **29,** 577–585
38. Etscheid, M., Hunfeld, A., König, H., Seitz, R., and Dodt, J. (2000) Activation of proPHBSP, the zymogen of a plasma hyaluronan binding serine protease, by an intermolecular autocatalytic mechanism. *Biol. Chem.* **381,** 1223–1231
39. Choi-Miura, N. H., Saito, K., Takahashi, K., Yoda, M., and Tomita, M.

(2001) Regulation mechanism of the serine protease activity of plasma hyaluronan binding protein. *Biol. Pharm. Bull.* **24,** 221–225
40. Nakazawa, F., Kannemeier, C., Shibamiya, A., Song, Y., Tzima, E., Schubert, U., Koyama, T., Niepmann, M., Trusheim, H., Engelmann, B., and Preissner, K. T. (2005) Extracellular RNA is a natural cofactor for the (auto-)activation of factor VII-activating protease (FSAP). *Biochem. J.* **385,** 831–838
41. Yamamichi, S., Nishitani, M., Nishimura, N., Matsushita, Y., and Hasumi, K. (2010) Polyamine-promoted autoactivation of plasma hyaluronan-binding protein. *J. Thromb. Haemost.* **8,** 559–566
42. Niu, W., Chen, Z., Gandhi, P. S., Vogt, A. D., Pozzi, N., Pelc, L. A., Zapata, F., and Di Cera, E. (2011) Crystallographic and kinetic evidence of allostery in a trypsin-like protease. *Biochemistry* **50,** 6301–6307
43. Abrams, S. T., Zhang, N., Manson, J., Liu, T., Dart, C., Baluwa, F., Wang, S. S., Brohi, K., Kipar, A., Yu, W., Wang, G., and Toh, C. H. (2013) Circulating histones are mediators of trauma-associated lung injury. *Am. J. Respir. Crit. Care Med.* **187,** 160–169